European Polymer Journal 119 (2019) 229–238

Contents lists available at ScienceDirect

European Polymer Journal

journal homepage: www.elsevier.com/locate/europolj

Amorphous to high crystalline PE made by mono and dinuclear Fe-based catalysts

Mostafa Khoshsefat[a,b,c,*], Abbas Dechal[b], Saeid Ahmadjo[b], S. Mohammad M. Mortazavi[b], Gholamhossein Zohuri[d], Joao B.P. Soares[a]

[a] Department of Chemical and Materials Engineering, University of Alberta, Edmonton, Alberta T6G 1H9, Canada
[b] Department of Catalyst, Iran Polymer and Petrochemical Institute (IPPI), P.O. Box 14965/115, Tehran, Iran
[c] Department of Polymer Engineering, Amirkabir University of Technology, P.O. Box 15785, Tehran, Iran
[d] Department of Chemistry, Faculty of Science, Ferdowsi University of Mashhad, P.O. Box 91775, Mashhad, Iran

ARTICLE INFO

Keywords:
Optimum bulkiness
Cocatalyst
Bridge
Amorphous
Structure-property relation

ABSTRACT

We designed a series of dinuclear structures (F_1–F_5) bearing different linkers (rigid to flexible) between the Fe centers to investigate that how they could control the catalyst behaviour and polymer properties. The dinculear structures were used for polymerization of ethylene in presence of MMAO and TiBA. Based on initial results, catalyst F_2 containing methyl-substituted phenyl bridge owned the highest activity (4.9×10^6 g PE/mol Fe.h) through dinuclearity and optimum bulkiness among the structures studied. This performance was along with the greatest crystallinity (χ_c) of PE made by the catalyst. Polymerization at higher temperature and monomer pressure exhibited high thermal stability and performance of catalyst F_2, respectively. For further structures, decreasing of effective electronic and steric features led to lower activity. In addition, not only catalyst F_4 bearing the short ethylene bridge exhibited the lowest productivity, but also produced the PE containing high level of short chain branches (37.2 SCB/1000C) affording a branched microstructure of polyethylene in presence of TiBA. It could attribute to low steric and electronic effects and short distance between the centers (ethylene linker) that made it suitable and active for SCB formation. Regarding to it, the electrophilicity index (ω) of F_4 also was greater that led to high capacity or propensity of the specie to accept the (macro) monomer. For this sample, virtually no χ_c observed in DSC and SSA thermograms. Moreover, MMAO acted as an effective cocatalyst in comparison to TiBA, according to the kinetic profiles of ethylene polymerization. The observations were in respect of strength and affinity of the cocatalysts in deactivation and reactivation of the centers at prolonged time.

1. Introduction

As the polyolefins microstructure has a key role on the physical and chemical properties of final product, the chemistry and structure of ligand and complex can control the catalyst behavior and polymer architecture [1–3]. This fact reveals the importance of structure design to reach desired properties [4–8]. There are many papers which have discussed about the catalyst structures from metal effect to ligand nature [9–11]. Late transition metals (LTM) complexes as a group of olefin polymerization catalyst have shown striking features. For instance; copolymerization of polar monomers, synthesis of linear to hyperbranched polyethylene, rare short chain branches formation and so on [12–20]. The chain walking mechanism for these structures is the main origin of the observed properties [17–20]. Multinuclear LTM catalysts are also interesting due to the unusual and unique pattern in the polymerization [10]. Among LTM complexes, imino pyridine Fe-based catalysts with high activity competitively to metallocenes are one of the fascinating structures that produce HDPE or oligomers [2,21,22]. This variety of products of bis(imino)pyridine iron based catalysts also is due to ortho-substituent effect and aryl rings that make the active center to produce polymer or oligomer and linear to branched (rarely) polyethylene [21,23]. Totally, catalyst structure lead to different behaviour of catalyst and thermal and microstructural properties of polymer. High activity and convenient working and ease synthesis of the mononuclear analogues made it to be interested by scientist to focus on the multinuclear ones. The nature of bridge between the centers is important as well as the length of it [24,25]. To clarify, the length and nature of bridge have influence on the catalyst activity, stability and

* Corresponding author.
E-mail address: Mostafa.Khoshsefat@ualberta.ca (M. Khoshsefat).

https://doi.org/10.1016/j.eurpolymj.2019.07.042
Received 14 June 2019; Received in revised form 25 July 2019; Accepted 30 July 2019
Available online 03 August 2019
0014-3057/

cooperation of the centers which may lead to effective interactions [2]. These features allow the catalysts to produce polyolefin with different microstructure and properties.

There are some similar reported structures where the results were notably interesting. Di, tri, tetra or even octanuclear Fe-based catalysts which activated by TiBA, MAO or MMAO, and showed some synergistic effects in comparison to mononuclear analogues [26–33]. Higher catalytic activity, lifetime, thermal stability of complexes along with the higher molecular weights (M_w), melting points (T_m), broader molecular weight distributions (MWD) and higher linearity features of PE are some of the observations in the literatures. The structures are bearing rigid to flexible bridge between the centers. However, it seemed that there is a need for a study on the nature of linker between the centers.

In addition to catalyst structure, the polymerization parameters are very effective to control the behaviors and properties. One of the most important parameters, which frequently discussed in the papers, is the cocatalyst [34,35]. The nature and concentration of cocatalyst are very crucial that make it to be a proper activator and impurity scavenger. One of the advantageous of iron catalysts is good responsibility to common alkyl activator such as TiBA instead of MAO or MMAO that makes it desirable for industrial application [36].

Herein, we investigated the effect of catalyst and cocatalyst natures and structures for polymerization of ethylene. Each parameter showed a specific influence on the catalyst behavior and produced polyethylene. Some theoretical factors also monitored to compare with experimental results. The catalysts behaviors were comprised through the nuclearity, nature and length of bridge between the centers and nature of the activator.

2. Experimental

2.1. Materials

All manipulations of air/water sensitive compounds were conducted under Ar/N_2 atmosphere using the standard Schlenk technique. All the solvents were purified prior to use. Toluene (purity 99.9%) was purified over sodium wire/benzophenone, and used as polymerization media and second step of ligand synthesis. Anhydrous THF obtained using the same procedure and it used in the synthesis of complexes. Methanol (Merck chemical) was purified over calcium hydride powder, and distilled prior to use in first step of ligand synthesis as solvent. Xylene was purchased from Merck chemical and used for purification of PE samples. 2,6- diisopropyl aniline, 1,4-phenylene diamine, 2,3,5,6-tetramethyphenyldiamine, ethylenediamine, 1,6-hexanediamine, 4,4′-methylenedianiline, 2,6-diacetyl pyridine, iron (II) dichloride and petroleum ether (purity 99.5%) were supplied by Merck Chemical (Darmstadt, Germany) and used in synthesis of ligands and complexes. Ethylene (purity 99.99%) was provided by Bandar Imam Petrochemical Company (BIPC, Iran). Modified-Methylaluminoxane (MMAO) (7 wt% in Toluene) and triisobutyl aluminium (TiBA) were supplied by Sigma Aldrich Chemicals (Steinheim, Germany).

2.2. Polymerization procedure

Ethylene polymerizations were conducted in a 200 mL stainless steel Buchi reactor, using toluene as the solvent. The reactor was purged with nitrogen at 90 °C for 2 h prior to each reaction. Dried toluene, cocatalyst and catalyst were introduced under nitrogen atmosphere, respectively. The reactor was saturated with ethylene to desired total pressure and reaction proceeded for 30 min, by mixing at 800 rpm. To better study on the reaction coordinate, the stirrer was stopped while injection of catalyst then stirrer and plot started, concurrently. Ethylene consumption was compensated using a mass flow meter to keep the pressure constant. Finally, the reactor was evacuated and the product was washed with acidic methanol (5%) and dried under reduced pressure.

2.3. Characterization

^{1}H NMR and FT-IR spectrums were obtained using Bruker AC-400 and Thermo Nicolet AVATAR 370 spectrometers, respectively. Elemental and Mass analyses were performed on a Thermo Finnigan Flash 1112EA microanalyzer and Varian CH-7A spectrometer. MWDs were determined with a Polymer Char high-temperature gel permeation chromatographer (GPC), run at 145 °C under a flow rate of 1,2,4-trichlorobenzene of 1 mL min^{-1}. The GPC was equipped with three detectors in series (infrared, light scattering, and differential viscometer) and calibrated with polystyrene narrow standards [31]. Differential scanning calorimetry (DSC) thermograms were recorded at second heating cycle with the rate of 10 °C/min by Perkin Elmer DSC Q100 instrument. Successive self-nucleation and annealing (SSA) analysis was carried out at the heating and cooling rates of 10 °C min^{-1}. Samples were first heated to 180 °C, maintained for 10 min, and cooled down to 25 °C. Subsequently, samples were heated to the first self-nucleation temperature (T1), maintained for 10 min then cooled down to 25 °C. Successive self-nucleation was achieved by repeatedly heating to the next self-nucleation temperatures and cooling down to 25 °C. After covering the temperature range between 165 and 25 °C, the final heating ramp from 25 up to 170 °C was applied to collect all melting endotherms [37].

2.4. Ligands and complexes synthesis

All the ligands (SIL_n, n = 1–6) and complexes (M_1 and F_n, n = 1–5) (Scheme 1) were synthesized and characterized which the spectrums are provided in the supporting information (SI) [25,39].

(E)-1-(6-(1-((2,6-diisopropylphenyl)imino)ethyl)pyridin-2-yl) ethan-1-one (SIM): To a solution of 2,6-diacetyl pyridine (10 mmol) and catalytic amount of formic acid in methanol (15 mL), 2,6-diisopropyl aniline (9 mmol) was added by dropping funnel at room temperature. The progress of reaction was measured by TLC technique. After 12 h, a pale yellow solid was filtered off and washed with cold methanol. For purification, the precipitate was suspended in refluxing ethanol, then filtered while still hot. The product was dried under reduced pressure (yield: 85%).^{1}HNMR ($CDCl_3$, 300 MHz): δ = 1.19 (6H, d), 1.23 (6H, d), 2.31 (3H, s), 2.84 (2H, sep), 2.90 (3H, s), 7.10–7.28 (3H, m), 8.07 (1H, t), 8.25 (1H, d), 8.65 (1H, d). Anal. Calcd. For $C_{21}H_{26}N_2O$: C, 78.22; H, 8.13; N, 8.69. Found: C, 78.27; H, 8.20; N, 8.12. Ft-IR (KBr, cm^{-1}): 1648 (−C═N−), 1699 (−C═O−). Mass (EI, *m/z*): 322 [M^+, 100%].

(1E,1′E)-1,1′-(pyridine-2,6-diyl)bis(N-(2,6-diisopropylphenyl) ethan-1-imine) (SIL_1): To a solution of 2,6-diisopropyl aniline (10 mmol) and 2,6-diacetyl pyridine (9 mmol), a catalytic amount of formic acid was added and then stirred for 12 h. The yellow product was filtered and washed with cold methanol. The solid dried under reduced pressure (yield: 98%). ^{1}HNMR ($CDCl_3$, 300 MHz): δ = 1.1 (24H, d), 2.2 (6H, s), 2.8 (4H, sep), 7.1 (6H, m), 7.9 (1, t), 8.5 (2, d). Anal. Calcd. For $C_{33}H_{43}N_3$: C, 82.28; H, 9.00; N, 8.72. Found: C, 82.43; H, 9.03; N, 8.39. Ft-IR (KBr, cm^{-1}): 1649 (−C═N−). Mass (EI, *m/z*): 481 [M^+, 100%].

(1E,1′E)-N,N'-(1,4-phenylene)bis(1-(6-((E)-1-((2,6-diisopropylphenyl)imino)ethyl)pyridin-2-yl)ethan-1-imine) (SIL_2): To a hot solution of SIM (15 mmol) in xylene, a solution of 1,4-phenylene diamine (7 mmol) was added in presence of para-toluene sulfonic acid as catalyst. The solution stirred for 72 h using Dean-Stark apparatus. The solution was cooled down and filtered. The solid was washed with cold methanol for several times.^{1}HNMR ($CDCl_3$, 300 MHz): δ = 1.20 (d, 12H), 1.21 (d, 12H), 2. 31 (s, 6H), 2.33 (s, 6H), 2.74–2.85 (m, 4H), 6.93(s, 4H), 7.12(t, 2H), 7.38 (d, 4H), 7.95 (t, 2H), 8.51 (d, 4H). Anal. Calcd. For $C_{48}H_{56}N_6$: C, 80.41; H, 7.87; N, 11.72. Found: C, 80.27; H, 7.70; N, 11.64. Ft-IR (KBr, cm^{-1}): 1642 (−C═N−). Mass (EI, *m/z*): 716 [M^+, 100%].

(1E,1′E)-N,N'-(2,3,5,6-tetramethyl-1,4-phenylene)bis(1-(6-((E)-

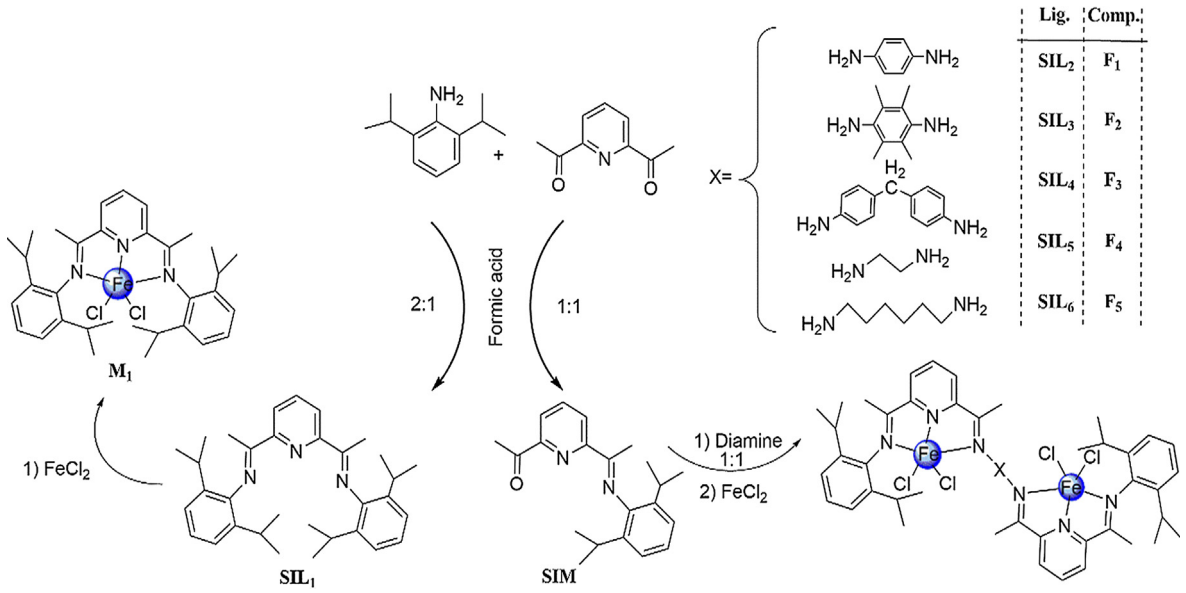

Scheme 1. Synthesis procedure of ligands and catalysts.

1-((2,6-diisopropylphenyl)imino)ethyl) pyridine-2-yl)ethan-1-imine) (SIL_3): The same procedure was employed for synthesis of SIL_3. ^{1}HNMR ($CDCl_3$, 300 MHz): δ = 1.17 (d, 12H), 1.19 (d, 12H), 2.24 (s, 12H), 2.33 (s, 6H), 2.34 (s, 6H), 2.74–2.80 (m, 4H), 7.14 (t, 2H), 7.31 (d, 4H), 7.99 (t, 2H), 8.59 (d, 4H). Anal. Calcd. For $C_{52}H_{64}N_6$: C, 80.79; H, 8.34; N, 10.87. Found: C, 80.70; H, 8.26; N, 10.67. Ft-IR (KBr, cm^{-1}): 1646 (−C═N−). Mass (EI, *m/z*): 772 [M^+, 100%].

(1E,1′E)-N,N'-(methylenebis(4,1-phenylene))bis(1-(6-((E)-1-((2,6-diisopropylphenyl)imino)ethyl)pyridin-2-yl)ethan-1-imine) (SIL_4): The same procedure was employed for synthesis of SIL_3. ^{1}HNMR ($CDCl_3$, 300 MHz): δ = 1.12–1.33 (m, 24H), 2.29 (s, 12H), 2.79 (m, 4H, 3.91 (s, 2H), 6.96–7.15 (m, 14H), 7.95 (t, 2H), 8.53 (m, 4H, H). Anal. Calcd. for $C_{55}H_{62}N_6$: C, 81.84; H, 7.74; N, 10.41. Found: C, 81.80; H, 7.74; N, 10.41. Ft-IR (KBr, cm^{-1}): 1644 (−C═N−). Mass (EI, *m/z*): 806 [M^+, 100%].

(1E,1′E)-N,N'-(ethane-1,2-diyl)bis(1-(6-((E)-1-((2,6-diisopropylphenyl)imino)ethyl)pyridin-2-yl)ethan-1-imine) (SIL_5): The same procedure was employed for synthesis of SIL_3. ^{1}HNMR ($CDCl_3$, 300 MHz): δ = 1.19 (d, 12H), 1.25 (d, 12H), 1.84 (t, 4H), 2.25 (s, 12H), 2.76 (m, 4H), 7.13 (t, 2H), 7.22 (d, 4H), 7.98 (t, 2H), 8.59 (d, 4H). Anal. Calcd. For $C_{44}H_{56}N_6$: C, 79.00; H, 8.44; N, 12.56. Found: C, 78.98; H, 8.29; N, 12.60. Ft-IR (KBr, cm^{-1}): 1632 (−C═N−). Mass (EI, *m/z*): 668 [M^+, 100%].

(1E,1′E)-N,N'-(hexane-1,6-diyl)bis(1-(6-((E)-1-((2,6-diisopropylphenyl)imino)ethyl)pyridin-2-yl)ethan-1-imine) (SIL_6): The same procedure was employed for synthesis of SIL_3. ^{1}HNMR ($CDCl_3$, 300 MHz): δ = 1.19 (d, 12H), 1.23 (d, 12H), 1.38 (m, 4H), 1.69 (m, 4H), 1.89 (t, 4H), 2.29 (s, 12H), 2.79 (m, 4H), 7.15 (t, 2H,), 7.23 (d, 4H), 7.99 (t, 2H), 8.63 (d, 4H,). Anal. Calcd. For $C_{48}H_{64}N_6$: C, 79.51; H, 8.90; N, 11.59. Found: C, 79.41; H, 8.81; N, 11.33. Ft-IR (KBr, cm^{-1}): 1638 (−C═N−). Mass (EI, *m/z*): 724 [M^+, 100%].

2.5. General procedure for synthesis and characterization of complexes

To a suspension of $FeCl_2$ (1.1 equiv.) in THF, a solution of ligand (SIL_1: 1.0 equiv. and SIL_n, n = 2–6: 0.5 equiv.) was added and refluxed for 10 min. The mixture then cooled down and filtered under nitrogen purge. The product was washed with THF and petroleum ether. Under stream of nitrogen, the solid was dried. All the solids were in blue and dark blue color.

The FT-IR spectrums of the complexes (provided in SI) revealed that the imine signal was shifted to weak field as it coordinated to the Fe atoms. This shift for M_1 was to 1619 cm^{-1}, while for dinuclear complexes were 1613, 1612, 1607, 1602 and 1615 cm^{-1} (from F_1 to F_5), respectively. Elemental analysis of the complexes, strongly, confirmed the structures which the difference between the theoretical and experimental values was less than 0.5%. Table of elemental analysis also are provided in the SI.

3. Results and discussion

3.1. Productivity and kinetic of polymerization

The dinuclear structures (F_n, n = 1–5) bearing rigid to flexible bridges along with the mononuclear (M_1) were used in the polymerization of ethylene using MMAO and TiBA as cocatalysts. The results are presented in Fig. 1 and Table 1. Catalyst F_2 through the optimum bulkiness around the active center showed the highest activity among the mono and dinuclear catalysts. The productivity of the catalysts was in the order of $F_2 > M_1 > F_5 > F_3 > F_4 > F_1$ in presence of MMAO and also the same trend was observed in presence of TiBA except $F_1 > F_4$. These trends are showing the importance of the ortho-aryl effect (i.e. M_1) and electron density delivered by the bridge between the centers (i.e. $F_5 > F_4$ and $F_3 > F_1$) [7,37,38,40–43]. These observations are consistent on our previous results on dinuclear Ni-based catalysts bearing the same bridges [7,37]. The effect of polymerization parameters such as [Al]/[Fe] molar ratio, temperature and monomer pressure on the catalyst behaviour and polymer properties was investigated. High concentration of TiBA (runs: 9, 11, 13, 16) led to higher performance of the catalysts that ascribed to reaching greater concentration of active centers [10,11]. Polymerization at higher temperature for catalyst F_2 revealed better performance, while the activity decreased after 65 °C. Increasing of kinetic energy of polymerization species along with the stability of the catalyst are the reasons for enhancing of productivity [10]. After 65 °C, irreversible deactivation and degradation of the catalyst as chemical factors and decreasing of monomer solubility as physical factor could interpret the observations [25,37]. M_w of the sample dropped by half and MWD was narrower (i.e. [Al]/[Fe] = 1500 and T_p = 65 °C; run 18) than the PE prepared at both lower TiBA concentration and polymerization temperature (i.e. [Al]/[Fe] = 1000 and T_p = r.t.; run 10). In this case, although, it was not clear that decreasing of M_w is mostly due to high cocatalyst concentration or polymerization temperature, it is accepted that the increasing of these factors increases the chain transfer and termination

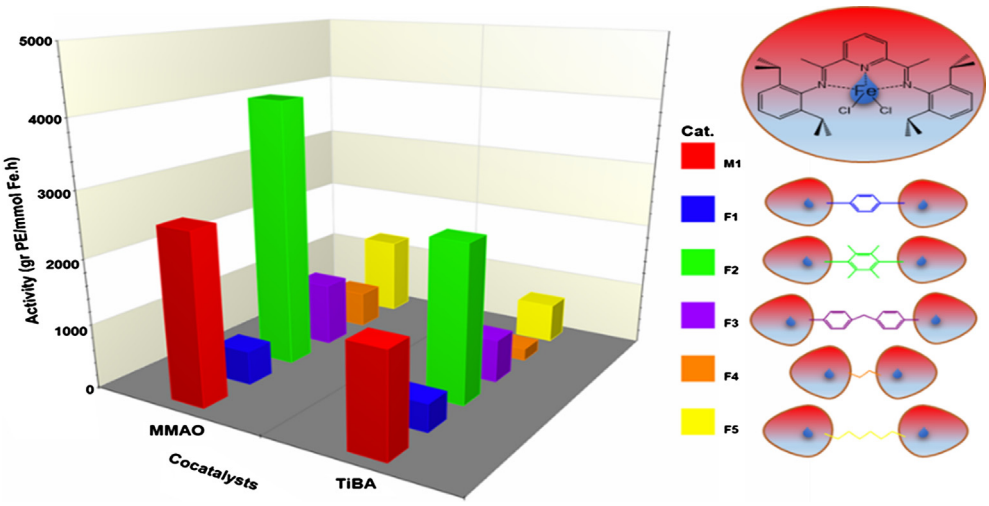

Fig. 1. Chart of ethylene polymerization results in presence of mono-(M_1) and dinuclear (F_n, n = 1–5) catalysts.

reactions affording lower M_w of the resultant polymer [26,44]. The productivity of catalyst F_2 and M_w of the sample also increased as the ethylene pressure augmented in the reactor. Besides, MWD of the polymer (run 20) slightly decreased. Increasing of monomer concentration and propagation/transfer or termination ratio controlled the catalyst behavior [10,43].

The kinetic profiles of ethylene polymerization using the catalysts in presence of MMAO and TiBA are depicted in Fig. 2. Higher monomer uptake and consumption by F_2 reflected the higher activity and stability, while for the further dinuclear structures; less shielding effects caused lower activity and stability. On the other hands, the difference between the catalyst behaviour against the different cocatalysts could be observed. By considering the deactivation and reactivation Eqs. (1) and (2), it could be proposed that MMAO acts much better for reactivation of center than TiBA due to its structure and higher Lewis acidity of Al [45–47].

$$C_t + Cocat \overset{k_d}{\rightarrow} C_d \quad (1)$$

$$C_d + Cocat \overset{k_{re}}{\rightarrow} C_t \quad (2)$$

3.2. Microstructure properties

The impact of catalyst and cocatalyst structures was not limited to the catalyst activity but also the final products affected by the nature and concentration of activator. One of the characteristics of iminopyridine iron based catalyst in polymerization of ethylene is production of HDPE with broad MWD at moderate reaction conditions [26,27,48]. Broadening of the MWD has been attributed to the presence of more than one active center due to different combination of catalyst and

Table 1
Results of ethylene polymerization using mono and dinuclear catalysts in presence of MMAO and TiBA.

Run	Cat.	Yield(g)	Activity (g PE/mmol Fe.h)	M_n[b] (g/mol)	M_w[b] (g/mol)	MWD[b]	T_m[a] (°C)	X_c[a] (%)	SCB/1000C[b]
1	M_1	5.5	2619.0	6600	143,000	21.7	137.0	67.8	5.5
2	F_1	1.1	523.8	5300	180,000	34.2	138.0	67.6	6.7
3	F_2	10.3	4904.8	8700	104,000	12.0	138.0	79.8	4.6
4	F_3	2.1	1000.0	3100	30,800	9.9	132.7	68.2	11.6
5	F_4	1.2	571.4	2000	30,700	15.6	128.5	60.9	16.6
6	F_5	2.6	1238.1	4400	98,700	22.3	137.6	64.8	7.8
7	M_1[c]	3.3	1571.4	5000	66,600	13.2	132.6	73.9	9.5
8	F_1[c]	0.7	333.3	2400	145,000	59.2	124.9	25.5	16.0
9	F_1[d]	0.9	428.6	n.d.	n.d.	n.d	121.6	27.3	n.d
10	F_2[c]	4.6	2190.5	4900	50,600	10.3	125.3	73.6	11.5
11	F_2[d]	5.1	2428.6	n.d	n.d	n.d	135.6	n.d	n.d
12	F_3[c]	0.8	381.0	2000	36,400	18.3	128.8	66.6	13.4
13	F_3[d]	1.4	666.7	n.d	n.d	n.d	129.8	65.0	n.d
14	F_4[c]	0.4	190.5	2900	24,000	8.3	–	0.0	37.2
15	F_5[c]	1.0	476.2	3000	45,300	14.9	133.8	25.8	21.3
16	F_5[d]	1.3	619.0	n.d	n.d	n.d	n.d	n.d	n.d
17	F_2[d,e]	6.1	2904.8	n.d	n.d	n.d	129.1	65.9	n.d
18	F_2[d,f]	6.3	3000.0	3800	24,600	6.4	128.3	66.1	12.8
19	F_2[d,g]	3.6	1714.3	n.d	n.d	n.d	126.6	61.5	n.d
20	F_2[d,h]	7.5	3571.4	5500	52,200	9.6	136.2	68.8	7.2

[a,b] obtained by DSC and high temperature GPC-IR instruments, respectively. Polymerization Condition: runs 1–6 were carried out in presence of MMAO while for 7–20 TiBA were used. [Fe]:4.2 μmol, [Al]/[Fe]:1000, ethylene pressure: 2 bar, toluene 80 mL, temperature: r.t., time: 30 min.
[c] [Al]/[Fe]: 1000.
[d] [Al]/Fe]:1500.
[e] 50 °C.
[f] 65 °C.
[g] 80 °C.
[h] 5 bar.

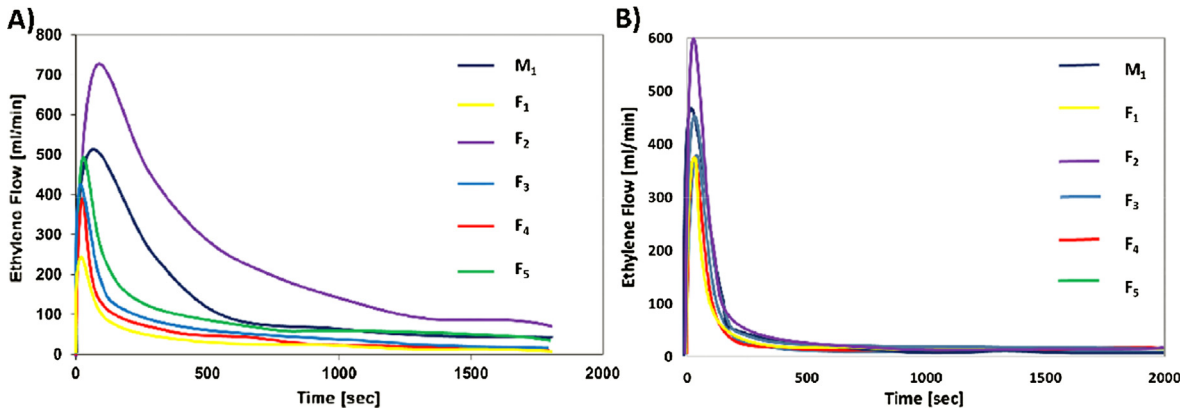

Fig. 2. Kinetic profiles of ethylene polymerization using mono (M_1) and dinculear (F_n, n = 1–5) catalysts in presence of (A) MMAO, (B) TiBA.

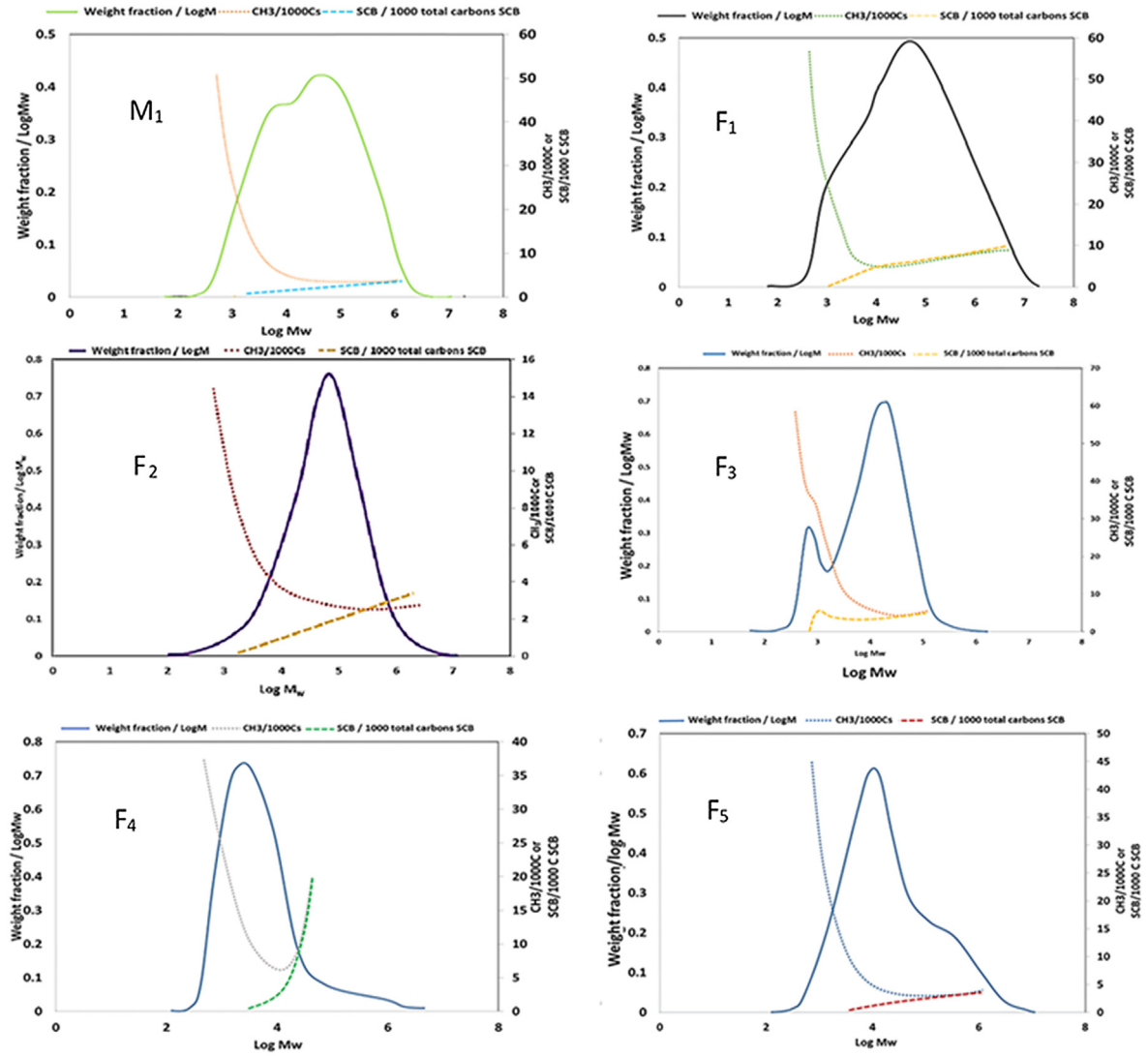

Fig. 3. The MWD and SCB curves of PE obtained by mono and dinuclear catalysts in presence of MMAO.

cocatalyst and reduction of initial active center to second one [26]. Moreover, it also has claimed that the more active (and unstable) centers operated at the early stages of polymerization, gradually transforming into the less active sites; the former sites afforded the low-M_W polyethylene fraction, while the latter sites were responsible for the higher- M_W PE fraction [22]. In the other side, unimodal molecular weight distribution has been reported for some mononuclear structures which strongly depends on the reaction conditions [22]. However, presence of different stereoisomers might be considered which is consistent on previous results of dinuclear catalysts [10,25]. Besides, it

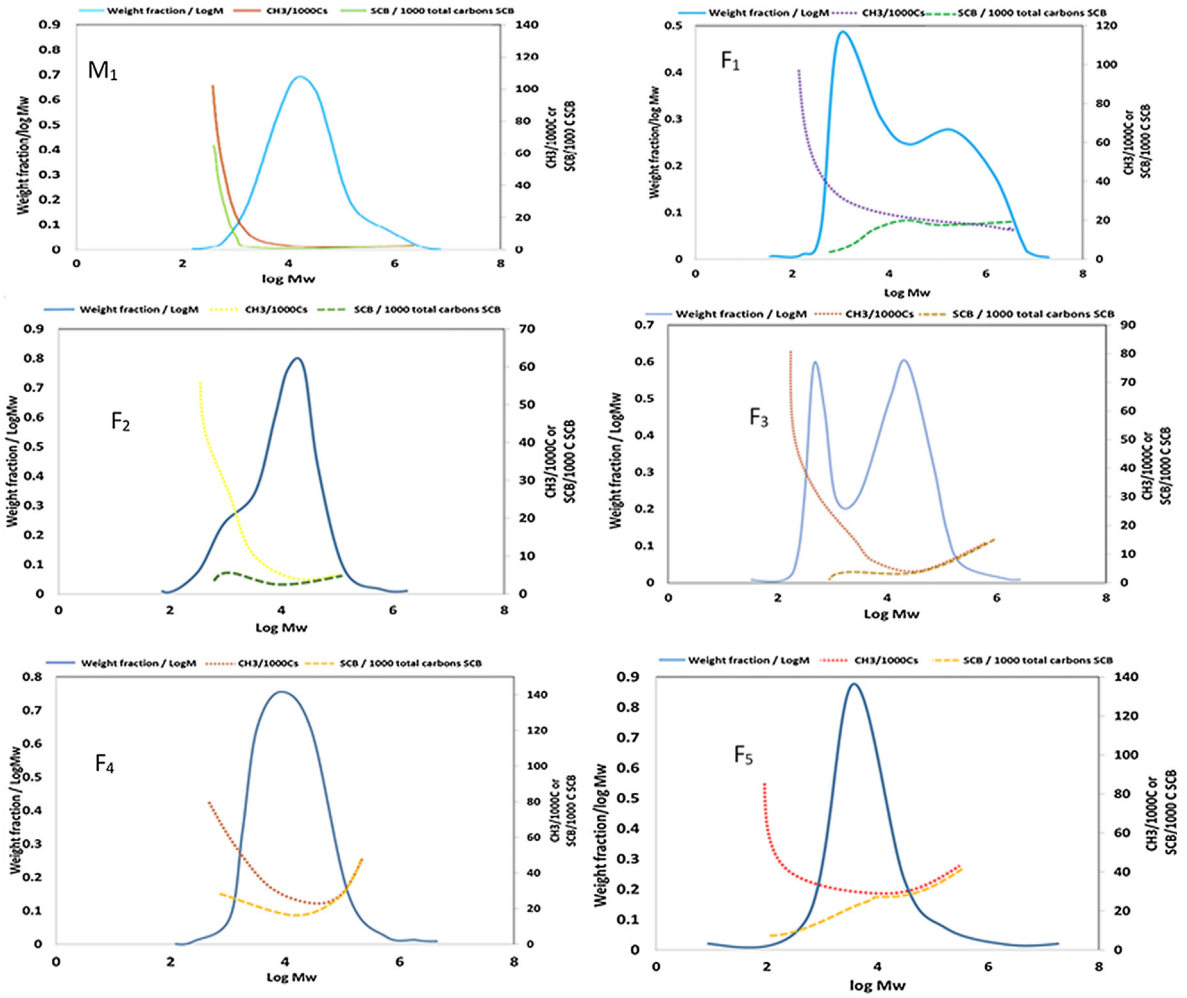

Fig. 4. The MWD and SCB curves of PE obtained by mono and dinuclear catalysts in presence of TiBA.

seems that both stereoisomers exist concurrently during the polymerization as catalysts are active in a very short time of polymerization in presence of TiBA. Different trends for SCB/1000C (Figs. 3 and 4) especially for cat/TiBA system implied the different behaviour of active centers. Moreover, in presence of TiBA, M_w and MWD decreased, while the SCB/1000C increased due to higher level of chain transfer reactions by TiBA (Fig. 4).

A proposed mechanism is depicted in Fig. 5. For dinuclear structures (except for F_4 and F_5), broadening to bimodality of MWD is much more obvious due to much difference between the activated sites leading low and high M_w fractions [25]. The GPC-IR graphs of the PE made by M_1 and F_2 using MMAO (Fig. 3) showed the higher M_w and narrow MWD for F_2 along with the slightly lower SCB/1000C. However, graph of CH_3/1000C revealed that higher level of methyl-end group for M_1 due to more fractions of low M_w. Electronic and steric effects are controlling factors of structure difference.

Based on this, by increasing these effects on the active centers, difference in catalyst structure and behaviour could be interpreted. For instance, catalyst F_4 bearing a short distance (higher steric effect than F_5) and lower electron density provided by ethylene bridge, showed the lowest activity and stability along with the highest SCB content.

However, by decreasing of bridge length, dinuclearity along with the catalyst…cocatalyst interactions increased. Furthermore, absence of bulky substituents and rigid structures for F_4 and F_5 open the structure orthogonal to N-N-N plane, and increase the frequency of the chain transfer reactions (molecular structures are provided in Fig. 6b (down) and SI) [21]. On the contrary, for catalyst M_1 and F_2, the situations are different (Fig. 6a (up) and SI). Study on the theoretical factors revealed that for catalyst F_4, high ω afforded high level of propensity or capacity of F_4 to accept the electrons (monomer or macromonomers) [49,50]. Due to low stability of the catalyst, it was active for a short time but produced PE containing high level of SCB.

These features could give the potential of chain transfer reactions and comonomer (macromonomer) incorporation. On the other hand, the extent of low M_w fractions for PE made by the catalysts is high where the values are 40–60 CH_3/1000C.

In respect of catalyst F_4, at first glance, it seems that adjacency of second metal center (figure S32, 6.16Å), very short energy interval between two stereoisomers and short lifetime have made the active centers to act similar but SCB/1000C graphs revealed different trends as it descends and ascends, respectively.

Based on proposed mechanism for activation and polymerization using TiBA, catalyst F_4 mostly goes through the route B including β–H elimination and 2,1-reinsertion which leads to high level of SCB. According to FT-IR spectra of the samples obtained in presence of TiBA (figures S27 and S28), absorbance of δ-CH_3 vibrations regarding the alkyl branches (methyl, ethyl and higher) at 1373, 1375 and 1378 cm^{-1} were strong for F_4 while the absorbance of δ-CH_2 vibrations attributing polymer chain backbone at 1462 and 1464 cm^{-1} were broad (due to amorphous phase) and weaker than further samples [51]. This amorphous phase also could be observed through the bands in the range of 715–735 cm^{-1} where the peaks were weak and negligible for F_4. These scenarios were the reverse for F_4 in presence of MMAO. Additionally, very weak absorbance of the band at 908 cm^{-1} related to

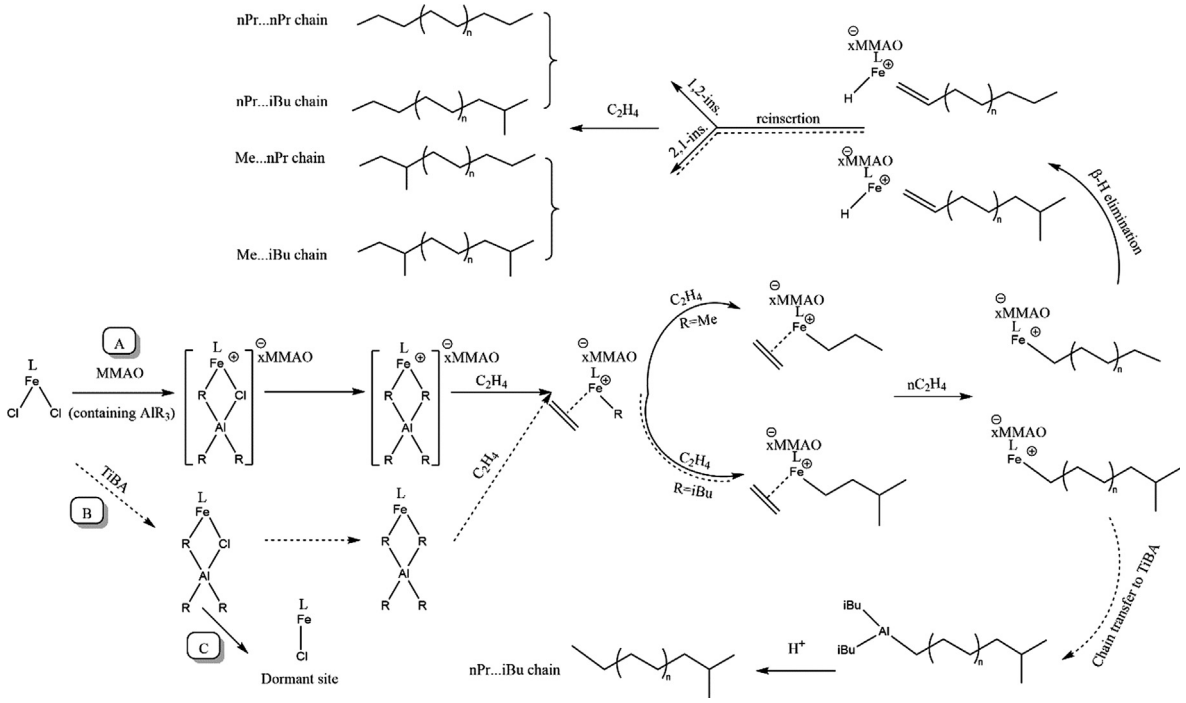

Fig. 5. Proposed mechanism for activation and ethylene polymerization by the catalysts in presence of MMAO and TiBA.

vinyl groups for F_1 and F_3 exhibited the effect of electronic and steric effects of structure and distance of active centers on the β–H elimination reaction. These bands were more obvious for samples made using TiBA due to dominating of β–H elimination during chain termination regarding the F_1 and F_3 catalyst structures (Fig. 5; route B).

3.3. Thermal properties

Crystallinities and melting points obtained by DSC thermograms of second heating cycle depicted in the Fig. 7and are in regard to the fractions made by each catalyst activated center and SCB content of them. The lowest SCB made by F_2 in presence of MMAO led to the highest χ_c while for F_4 in presence of TiBA, the highest SCB per 1000 carbon atoms and no χ_c were observed. In contrast, using MMAO led to high χ_c (60.9%) disclosed lower branches (route A; nPr chain and low Me branch content) than TiBA as the GPC-IR confirmed the results. Moreover, there are two endotherms for F_1 as it produced PE with a distinct bimodal distribution and different trends of SCB content for low and high M_w fractions. For the rest dinuclear catalysts, the same behaviour was observed. Lower melting temperatures of PE observed for all catalysts in presence of TiBA are in respect of thinner lamellae due to higher level of branches and shorter polymer chains. Due to low SCB/1000C of the polymer made by the most catalysts, it not showed a satisfactory fractionation in SSA thermograms (Fig. 8). Of course, there are some contributions for the main peaks, but the crystallinity domains were very close and the deconvolutions were not successful, accordingly. However, for the Cat/TiBA catalyst systems, there are some contributions at lower temperature than main T_m. All these observations showed that using TiBA leads to higher SCB formation.

4. Conclusion

Optimum bulkiness around the active center leading to desired steric and electronic effects along with the dinuclearity in catalyst F_2that played a key role on activity and stability. In addition to the greater performance of catalyst F_2, higher M_w and linearity feature of PE was obtained in comparison to the mono and further dinuclear structures. In contrast, catalyst F_4 through less hindrance and specific

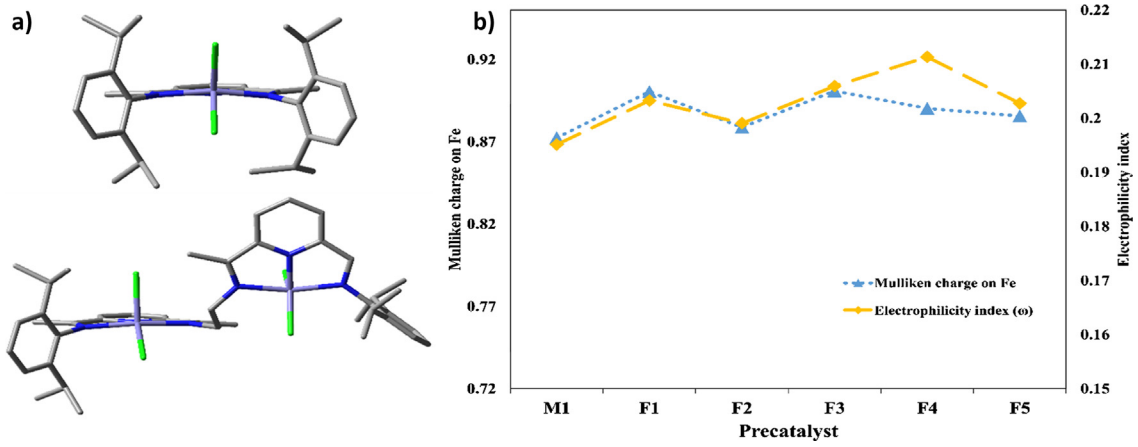

Fig. 6. (a) Molecular structures of precatalysts M_1 (up) and F_4 (down), (b) Theoretical factors calculated for the mono and dinuclear precatalysts.

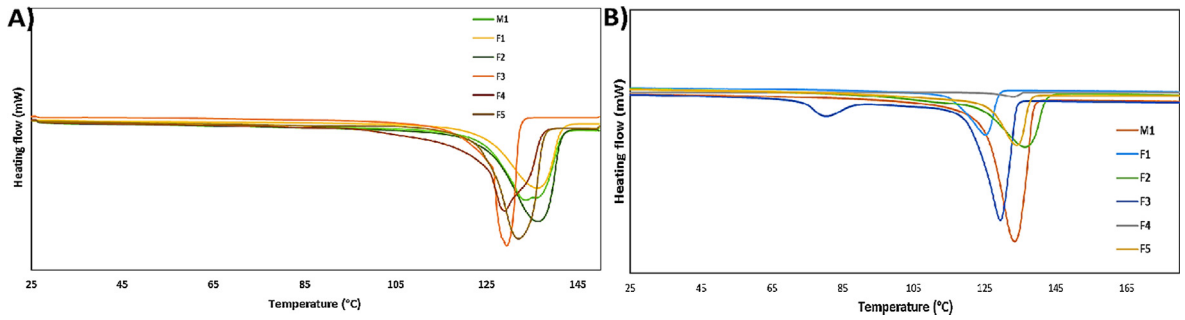

Fig. 7. DSC thermograms of PE made by mono and dinuclear catalysts in presence of (A) MMAO and (B) TiBA.

steric influence and electronic effect along with the short and no bulky group of the bridge between the centers produced a branched (an amorphous) PE with low activity in presence of TiBA. The molecular models and theoretical factors (i.e. electrophilicity and Mullikan charge) confirmed the experimental results. On the other hand, the effect of cocatalyst nature (i.e. MMAO and TiBA) was striking. Kinetic profiles of ethylene polymerization using the structures in presence of MMAO and TiBA, completely, revealed that MMAO acts as an effective activator. Strength and stability of the cocatalysts in deactivation and reactivation of the centers were controlling factors on catalyst behaviour at prolonged time. The impacts of polymerization conditions on catalyst behaviour and polymer properties were considerable.

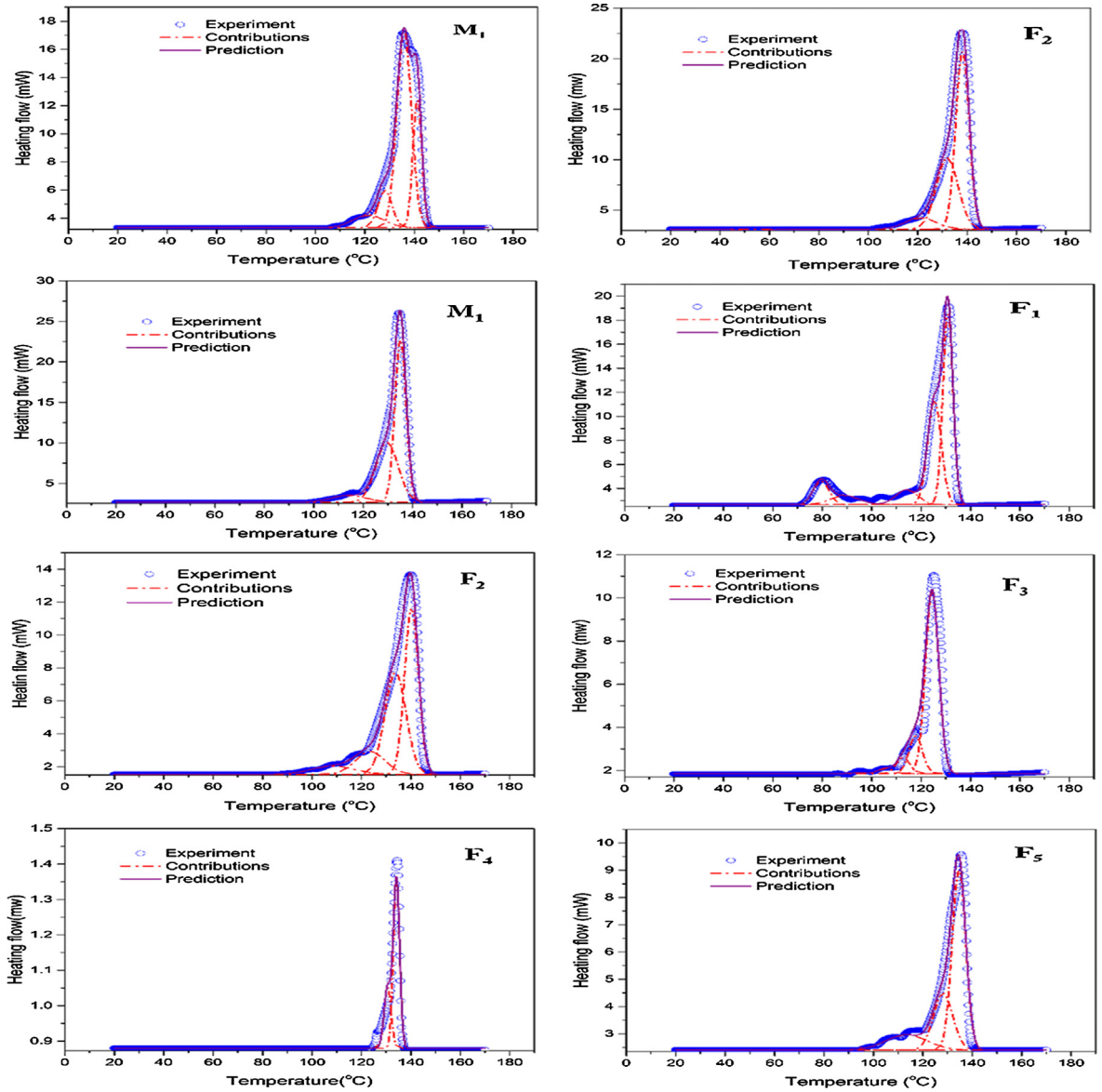

Fig. 8. SSA thermograms of PEs made by mono (M1) and dinuclear (F2) catalysts in presence of MMAO (top; left and right) and all mono and dinucleear structures in presence of TiBA.

Acknowledgment

The authors are thankful of University of Alberta (U of A), Iran Polymer and Petrochemical Institute (IPPI) and Ferdowsi university of Mashhad (FUM) for all their cooperation.

Appendix A. Supplementary material

Supplementary data to this article can be found online at https://doi.org/10.1016/j.eurpolymj.2019.07.042.

References

[1] G.H. Zohuri, S.M. Seyedi, R. Sandaroos, S. Damavandi, A. Mohammadi, Novel late transition metal catalysts based on iron: synthesis, structures and ethylene polymerization, Catal. Lett. 140 (2010) 160–166, https://doi.org/10.1007/s10562-010-0433-x.
[2] M. Delferro, T.J. Marks, Multinuclear olefin polymerization catalysts, Chem. Rev. 111 (2011) 2450–2485, https://doi.org/10.1021/cr1003634.
[3] N.V. Kulkarni, T. Elkin, B. Tumaniskii, M. Botoshansky, L.J.W. Shimon, M.S. Eisen, Asymmetric bis(formamidinate) group 4 complexes: synthesis, structure and their reactivity in the polymerization of α-olefins, Organometallics 33 (2014) 3119–3136, https://doi.org/10.1021/om500345r.
[4] F.S. Liu, H. Bin Hu, Y. Xu, L.H. Guo, S.B. Zai, K.M. Song, H.Y. Gao, L. Zhang, F.M. Zhu, Q. Wu, Thermostable α-diimine nickel(II) catalyst for ethylene polymerization: effects of the substituted backbone structure on catalytic properties and branching structure of polyethylene, Macromolecules 42 (2009) 7789–7796, https://doi.org/10.1021/ma9013466.
[5] F. Liu, H. Gao, Z. Hu, H. Hu, F. Zhu, Q. Wu, Poly(1-hexene) with long methylene sequences and controlled branches obtained by a thermostable α-diimine nickel catalyst with bulky camphyl backbone, J. Polym. Sci. Part A Polym. Chem. 50 (2012) 3859–3866, https://doi.org/10.1002/pola.26181.
[6] S. Kong, K. Song, T. Liang, C.-Y. Guo, W.-H. Sun, C. Redshaw, Methylene-bridged bimetallic α-diimino nickel(ii) complexes: synthesis and high efficiency in ethylene polymerization, Dalt. Trans. 42 (2013) 9176–9187, https://doi.org/10.1039/c3dt00023k.
[7] M. Khoshsefat, A. Dechal, S. Ahmadjo, Synthesis of poly(α-olefins) containing rare short-chain branches by dinuclear Ni-based catalysts, New. J. Chem. 42 (2018) 18288–18296, https://doi.org/10.1039/c8nj04481c.
[8] K. Lian, Y. Zhu, W. Li, S. Dai, C. Chen, Direct synthesis of thermoplastic polyolefin elastomers from nickel-catalyzed ethylene polymerization, Macromolecules 50 (2017) 6074–6080, https://doi.org/10.1021/acs.macromol.7b01087.
[9] A. Krasuska, M. BiaŁek, K. Czaja, Ethylene polymerization with FI complexes having novel phenoxy-imine ligands: effect of metal type and complex immobilization, J. Polym. Sci. Part A Polym. Chem. 49 (2011) 1644–1654, https://doi.org/10.1002/pola.24589.
[10] M. Khoshsefat, G.H. Zohuri, N. Ramezanian, S. Ahmadjo, M. Haghpanah, Polymerization of ethylene using a series of binuclear and a mononuclear Ni (II)-based catalysts, J. Polym. Sci. Part A Polym. Chem. 54 (2016) 3000–3011, https://doi.org/10.1002/pola.28186.
[11] M. Khoshsefat, N. Beheshti, G.H. Zohuri, S. Ahmadjo, S. Soleimanzadegan, Practical and theoretical study on the α-substituent effect on α-diimine Nickel(II) and Cobalt (II)-based catalysts for polymerization of ethylene, Polym. Sci. Ser. B. 58 (2016) 1–8, https://doi.org/10.1134/S1560090416050067.
[12] M. Stürzel, S. Mihan, R. Mülhaupt, From multisite polymerization catalysis to sustainable materials and all-polyolefin composites, Chem. Rev. 116 (2016) 1398–1433, https://doi.org/10.1021/acs.chemrev.5b00310.
[13] L. Guo, S. Dai, X. Sui, C. Chen, Palladium and nickel catalyzed chain walking olefin polymerization and copolymerization, ACS Catal. 6 (2016) 428–441, https://doi.org/10.1021/acscatal.5b02426.
[14] L. Guo, W. Liu, C. Chen, Late transition metal catalyzed α-olefin polymerization and copolymerization with polar monomers, Mater. Chem. Front. 1 (2017) 2487–2494, https://doi.org/10.1039/C7QM00321H.
[15] M. Chen, C. Chen, Rational design of high-performance phosphine sulfonate nickel catalysts for ethylene polymerization and copolymerization with polar monomers, ACS Catal. 7 (2017) 1308–1312, https://doi.org/10.1021/acscatal.6b03394.
[16] C.J. Stephenson, J.P. McInnis, C. Chen, M.P. Weberski, A. Motta, M. Delferro, T.J. Marks, Ni(II) phenoxyiminato olefin polymerization catalysis: striking coordinative modulation of hyperbranched polymer microstructure and stability by a proximate sulfonyl group, ACS Catal. 4 (2014) 999–1003, https://doi.org/10.1021/cs500114b.
[17] F. Wang, C. Chen, A continuing legend: the Brookhart-type α-diimine nickel and palladium catalysts, Polym. Chem. 10 (2019) 2354–2369, https://doi.org/10.1039/C9PY00226J.
[18] F. Wang, R. Tanaka, Z. Cai, Y. Nakayama, T. Shiono, Synthesis of highly branched polyolefins using phenyl substituted α-diimine Ni (II) catalysts, Polymers 8 (2016) 160, https://doi.org/10.3390/polym8040160.
[19] F. Wang, R. Tanaka, Q. Li, Y. Nakayama, T. Shiono, Chain-walking polymerization of linear internal octenes catalyzed by α-diimine nickel complexes, Organometallics 37 (2018) 1358–1367, https://doi.org/10.1021/acs.organomet.8b00042.
[20] M. Zhang, Q. Wu, G. Xu, Y. Li, F. Wang, Cationic para-phenyl-substituted α-diimine nickel catalyzed ethylene and 4-methyl-1-pentene (co) polymerizations via living/controlled chain-walking, Appl. Organomet. Chem. 33 (2019) e4911, https://doi.org/10.1002/aoc.4911.
[21] C. Bianchini, G. Giambastiani, I.G. Rios, G. Mantovani, A. Meli, A.M. Segarra, Ethylene oligomerization, homopolymerization and copolymerization by iron and cobalt catalysts with 2,6-(bis-organylimino)pyridyl ligands, Coord. Chem. Rev. 250 (2006) 1391–1418, https://doi.org/10.1016/j.ccr.2005.12.018.
[22] N.V. Semikolenova, W. Sun, I.E. Soshnikov, M.A. Matsko, O.V. Kolesova, V.A. Zakharov, K.P. Bryliakov, Origin of " Multisite-like " ethylene polymerization behavior of the single-site nonsymmetrical bis (imino) pyridine iron (II) complex in the presence of modified methylaluminoxane, ACS Catal. 7 (2017) 2468–2477, https://doi.org/10.1021/acscatal.7b00486.
[23] A.S. Abu-Surrah, K. Lappalainen, New bis (imino) pyridine-iron (II)-and cobalt (II)-based catalysts: synthesis, characterization and activity towards polymerization of ethylene, J. Organomet. Chem. 648 (2002) 55–61, https://doi.org/10.1016/S0022-328X(01)01418-8.
[24] R. Zhang, Z. Wang, Z. Flisak, X. Hao, Q. Liu, W.H. Sun, Achieving branched polyethylene waxes by aryliminocycloocta[b]pyridylnickel precatalysts: synthesis, characterization, and ethylene polymerization, J. Polym. Sci. Part A Polym. Chem. 55 (2017) 2601–2610, https://doi.org/10.1002/pola.28653.
[25] M. Khoshsefat, S. Ahmadjo, S.M.M. Mortazavi, G.H. Zohuri, J.B.P. Soares, Synthesis of low to high molecular weight poly(1-hexene); rigid/flexible structures in a di- and mononuclear Ni-based catalyst series, New. J. Chem. 42 (2018) 8334–8337, https://doi.org/10.1039/c8nj01678j.
[26] L. Wang, J. Sun, Methylene bridged binuclear bis(imino)pyridyl iron(II) complexes and their use as catalysts together with Al(i-Bu)3 for ethylene polymerization, Inorganica Chim. Acta. 361 (2008) 1843–1849, https://doi.org/10.1016/j.ica.2007.09.039.
[27] S. Zhang, W.H. Sun, X. Kuang, I. Vystorop, J. Yi, Unsymmetric bimetal(II) complexes: Synthesis, structures and catalytic behaviors toward ethylene, J. Organomet. Chem. 692 (2007) 5307–5316, https://doi.org/10.1016/j.jorganchem.2007.08.020.
[28] S. Zhang, I. Vystorop, Z. Tang, W.-H. Sun, Bimetallic (iron or cobalt) complexes bearing 2-methyl-2,4-bis(6-iminopyridin-2-yl)-1 h -1,5-benzodiazepines for ethylene reactivity, Organometallics 26 (2007) 2456–2460, https://doi.org/10.1021/om070062z.
[29] J. Liu, Y. Li, J. Liu, Z. Li, Ethylene polymerization with a highly active and long-lifetime macrocycle trinuclear 2,6-bis(imino)pyridyliron, Macromolecules 38 (2005) 2559–2563, https://doi.org/10.1021/ma047685y.
[30] Z.J. Zheng, J. Chen, Y.S. Li, The synthesis and catalytic activity of poly(bis(imino) pyridyl) iron(II) metallodendrimer, J. Organomet. Chem. 689 (2004) 3040–3045, https://doi.org/10.1016/j.jorganchem.2004.06.053.
[31] A.P. Armitage, Y.D.M. Champouret, H. Grigoli, J.D.A. Pelletier, K. Singh, G.A. Solan, Probing the effect of binding site and metal centre variation in pentadentate oligopyridylimine-bearing bimetallic (Fe_2, Co_2, Ni_2) ethylene oligomerisation catalysts, Eur. J. Inorg. Chem. 29 (2008) 4597–4607, https://doi.org/10.1002/ejic.200800650.
[32] P. Barbaro, C. Bianchini, G. Giambastiani, I.G. Rios, A. Meli, W. Oberhauser, A.M. Segarra, L. Sorace, A. Toti, C. Organometallici, V. Madonna, S.F. Firenze, D. Chimica, U. Instm, V. Uni, V. Lastruccia, S.F. Firenze, R.V. May, Synthesis of new polydentate nitrogen ligands and their use in ethylene polymerization in conjunction with iron (II) and cobalt (II) bis-halides and methylaluminoxane, Organometallics 26 (4639–4651) (2007) 4639–4651, https://doi.org/10.1021/om7005062.
[33] D. Takeuchi, S. Takano, Y. Takeuchi, K. Osakada, Ethylene polymerization at high temperatures catalyzed by double- decker-type dinuclear iron and cobalt complexes: dimer effect on stability of the catalyst and polydispersity of the product, Organometallics 33 (2014) 5316–5323, https://doi.org/10.1021/om500629a.
[34] A. Dechal, M. Khoshsefat, S. Ahmadjo, S.M.M. Mortazavi, G.H. Zohuri, H. Abedini, Mono-and binuclear nickel catalysts for 1-hexene polymerization, Appl. Organomet. Chem. 32 (2018) e4355, https://doi.org/10.1002/aoc.4355.
[35] R. Cheng, Z. Liu, L. Zhong, X. He, P. Qiu, M. Terano, M.S. Eisen, S.L. Scott, B. Liu, Polyolefins: 50 years after Ziegler and Natta, Advances in Polymer Science. New York, 2013.
[36] R. Hoff, R.T. Mathers, Handbook of Transition Metal Polymerization Catalysts, John Wiley & Sons, New Jersey, 2010.
[37] M. Khoshsefat, A. Dechal, S. Ahmadjo, S.M.M. Mortazavi, G. Zohuri, J.B. Soares, Cooperative effect through different bridges in nickel catalysts for polymerization of ethylene, Appl. Organomet. Chem. 33 (2019) e4929. https://doi.org/10.1002/aoc.4929.
[38] S.K. Noh, J. Kim, J. Jung, C.S. Ra, D. Lee, H.B. Lee, S.W. Lee, W.S. Huh, Syntheses of polymethylene bridged dinuclear zirconocenes and investigation of their polymerisation activities, J. Organomet. Chem. 580 (1999) 90–97, https://doi.org/10.1016/S0022-328X(98)01085-7.
[39] C. Bianchini, G. Mantovani, A. Meli, F. Migliacci, F. Zanobini, F. Laschi, A. Sommazzi, Oligomerisation of ethylene to linear α-olefins by new Cs-and C1-symmetric [2, 6-bis (imino) pyridyl] iron and-cobalt dichloride complexes, Eur. J. Inorg. Chem. 8 (2003) 1620–1631, https://doi.org/10.1002/ejic.200390213.
[40] G. Tian, B. Wang, S. Xu, X. Zhou, B. Liang, L. Zhao, F. Zou, Y. Li, Ethylene polymerization with sila-bridged dinuclear zirconocene catalysts, Macromol. Chem. Phys. 203 (2002) 31–36, https://doi.org/10.1002/1521-3935(20020101)203:1<31::AID-MACP31>3.0.CO;2-L.
[41] X. Xiao, J. Sun, X. Li, H. Li, Y. Wang, Binuclear titanocenes linked by the bridge combination of rigid and flexible segment: Synthesis and their use as catalysts for ethylene polymerization, J. Mol. Catal. A Chem. 267 (2007) 86–91, https://doi.org/10.1016/j.molcata.2006.11.025.
[42] S.K. Noh, J. Lee, D.H. Lee, Syntheses of dinuclear titanium constrained geometry

complexes with polymethylene bridges and their copolymerization properties, J. Organomet. Chem. 667 (2003) 53–60, https://doi.org/10.1016/S0022-328X(02)02125-3.
[43] G.J.P. Britovsek, M. Bruce, V.C. Gibson, B.S. Kimberley, P.J. Maddox, S. Mastroianni, S.J. McTavish, C. Redshaw, G.A. Solan, S. Strömberg, A.J.P. White, D.J. Williams, Iron and cobalt ethylene polymerization catalysts bearing 2,6-bis(imino)pyridyl ligands: synthesis, structures, and polymerization studies, J. Am. Chem. Soc. 121 (1999) 8728–8740, https://doi.org/10.1021/ja990449w.
[44] Qifeng Xing, Tong Zhao, Yusen Qiao, Lin Wang, Carl Redshaw, Wen-Hua Sun, Synthesis, characterization and ethylene polymerization behavior of binuclear iron complexes bearing N,N′-bis(1-(6-(1-(arylimino)ethyl) pyridin-2-yl)ethylidene)benzidines, RSC Adv. 3 (48) (2013) 26184, https://doi.org/10.1039/c3ra42631a.
[45] S. Mehdiabadi, J.B.P. Soares, Ethylene homopolymerization kinetics with a constrained geometry catalyst in a solution reactor, Macromolecules 45 (2012) 1777–1791, https://doi.org/10.1021/ma202577n.
[46] M. Khoshsefat, S. Ahmadjo, S.M.M. Mortazavi, G.H. Zohuri, Reinforcement effects of nanocarbons on catalyst behaviour and polyethylene properties through in situ polymerization, RSC Adv. 6 (2016) 88625–88632, https://doi.org/10.1039/C6RA16243F.
[47] R. Tanaka, T. Hirose, Y. Nakayama, T. Shiono, The preparation of boron-containing aluminoxanes and their application as cocatalysts in the polymerization of olefins, Polym. J. 48 (2015) 67–71, https://doi.org/10.1038/pj.2015.81.
[48] V.C. Gibson, C. Redshaw, G.A. Solan, Bis(imino)pyridines: surprisingly reactive ligands and a gateway to new families of catalysts, Chem. Rev. 107 (2007) 1745–1776, https://doi.org/10.1021/cr068437y.
[49] A. Vektariene, G. Vektaris, J. Svoboda, A theoretical approach to the nucleophilic behavior of benzofused thieno [3, 2-b] furans using DFT and HF based reactivity descriptors, Online. J. Organ. Chem 7 (2009) 311–329, https://doi.org/10.3998/ark.5550190.0010.730.
[50] R.G. Parr, C. Hill, N. Carolina, R.V. October, V. Re, M. Recei, V. December, Electrophilicity index, J. Am. Chem. Soc. 121 (1999) 1922–1924, https://doi.org/10.1021/ja983494x.
[51] H. Hagemam, R.G. Snyder, Quantitative infrared methods for the measurement of crystallinity and its temperature dependence: polyethylene, Macromolecul. 22 (1989) 3600–3606, https://doi.org/10.1021/ma00199a017.